Les Figs. (3)–(4) représentent respectivement pour: $Pr = 10^{-2}$; 0,7; 10; 10^2 les variations de $Nu. Re^{-1/2}$ et celles de $\frac{1}{2}C_f . Re^{1/2}$ en fonction de ξ déduites de (34)–(35) (approximation du 2nd ordre).

Insistons sur le fait que ces résultats ne sont valables que pour $\xi \ll 1$.

BIBLIOGRAPHIE

1. E. M. Sparrow, R. Eichorn and J. C. Gregg, Combined forced and free convection in a boundary layer flow, *Phys. Fluids* **2**, 319–328 (1959).
2. J. R. Kliegel, Laminar free and forced convective heat transfer from a vertical flat plate. Ph.D. thesis, University of California (1959).
3. J. H. Merkin, The effect of buoyancy forces on the boundary layer flow over a semi-finite vertical flat plate in a uniform free stream. *J. Fluid Mech.* **35**, 439–450 (1969).
4. J. R. Lloyd and E. M. Sparrow, Combined forced and free convection flow on vertical surfaces. *Int. J. Heat Mass Transfer* **13**, 434–438 (1970).
5. T. T. Kao, G. A. Domoto and H. G. Eirod, Jr., Free convection along a nonisothermal vertical flat plate. *Trans. ASME* 72–78 (1977).
6. A. A. Szewczyk, Combined forced and free-convection laminar flow. *J. Heat Transfer* 501–506 (1964).
7. A. Mucoglu and T. S. Chen, Mixed convection on a horizontal plate with uniform surface heat flux. *Proc. 6th Int. Heat Transfer Conf.*, Toronto, p. 85 (1978).
8. L. Lapidus and J. H. Seinfeld, *Numerical Solution of Ordinary Differential Equations*. Academic Press, N.Y. (1971).
9. M. H. Rogers and C. N. Lance, Flow in the presence of a rotating disk. *J. Fluid Mech.* **7**, 617–631 (1960).

Int. J. Heat Mass Transfer. Vol. 25, No. 7, pp. 1065–1069, 1982
Printed in Great Britain

0017-9310/82/071065-05 $03.00/0
Pergamon Press Ltd.

LAMINAR VISCO-ELASTIC FLOW AND HEAT TRANSFER BETWEEN TWO STATIONARY UNIFORMLY POROUS DISCS OF DIFFERENT PERMEABILITY

JYOTIRMOY SINHA ROY and NALIN KANTA CHAUDHURY

Post-Graduate Department of Mathematics, Utkal University, Vani Vihar, Bhubaneswar-751004, Orissa, India

(*Received* 1 *February* 1981 *and in revised form* 23 *October* 1981)

NOMENCLATURE

$2a$,	channel width;
E,	Eckert number;
$f(\eta), f'(\eta)$,	functions defined in (4);
$f_0(\eta), f_1(\eta), f_2(\eta)$,	functions defined in (7);
p,	pressure;
P,	Prandtl number;
q,	Nusselt number;
r_0,	the distance of a given point on either disc from the centre;
r,	dimensionless radial distance;
r', θ', z',	cylindrical polar coordinates;
R,	Reynolds number;
S,	elastic parameter;
T_1, T_2,	constant temperatures at the discs;
u', v',	velocity components in r', z' directions respectively;
u, v,	dimensionless velocity components;
V_1, V_2,	constant velocities at the discs.

Greek symbols

η,	dimensionless axial distance;
θ,	dimensionless temperature;
$\theta_0(\eta), \theta_2(\eta)$,	functions defined in (12);
λ,	the ratio of r by r_0;
τ,	dimensionless skin friction;
ϕ,	dissipation function.

1. INTRODUCTION

PROBLEMS of flow and heat transfer between two parallel porous or non-porous discs are of great importance in the design of thrust bearings, radial diffusers etc. Elkouh [1], Mishra *et al.* [2], Rasmussen [3] and Wang [4] studied a few problems between two rotating porous discs. All these authors confined their discussions to either constant suction or equal rates of suction and injection at the discs. Terril and Cornish [5] studied the problem of radial flow of a viscous, incompressible fluid between two stationary, uniformly porous discs of different permeability and obtained solutions for small as well as large suction and injection velocities. The purpose of this paper is to generalize Terril and Cornish's [5] problem to visco-elastic fluid and to study related heat transfer problem. Since the visco-elastic fluids are being used as lubricants this problem may be useful in the design of the externally pressurized thrust bearings. The visco-elastic fluid model considered is given by Walters [6].

2. MATHEMATICAL ANALYSIS

Consider the fluid in between two infinite porous discs $z' = -a$ and $z' = a$. The fluid is injected or sucked normally with constant velocity V_1 at $z' = -a$ and V_2 at $z' = a$. These velocities may have either sign but will be assumed positive in positive z'-direction. The discs are maintained at constant temperatures T_1 and T_2 respectively. The geometry of the problem is shown in the Fig. 1. We shall work through cylindrical polar system of coordinates (r', θ', z'). Let u' and v' represent the velocity components in the directions r' and z' respectively.

The momentum and the energy equations are

$$f'^2 - 2ff'' + \frac{2}{R}f''' = -\frac{4}{\rho r}\frac{\partial p}{\partial r} - S[4f'f''' - 2ff^{4'} + 2f''^2] \quad (1)$$

$$ff' = -\frac{1}{\rho}\frac{\partial p}{\partial \eta} + \frac{1}{R}f'' - S[ff''' - 3f'f''] \quad (2)$$

$$u\frac{\partial \theta}{\partial r} + v\frac{\partial \theta}{\partial \eta} = \frac{1}{PR}\left(\frac{\partial^2 \theta}{\partial r^2} + \frac{1}{r}\frac{\partial \theta}{\partial r} + \frac{\partial^2 \theta}{\partial \eta^2}\right) + \phi \quad (3)$$

where

$$r = \frac{r'}{a},\ \eta = \frac{z'}{a},\ u = \frac{u}{U_0},\ v = \frac{v'}{U_0},\ \theta = \frac{T - T_1}{T_2 - T_1},\ R = \frac{U_0 a}{\nu},$$

$$P = \frac{\eta_0 c}{k},\ E = \frac{U_0^2}{c(T_2 - T_1)},\ S = \frac{k_0^*}{a^2}.$$

U_0 is the characteristic velocity, ϕ is the dissipation function and

$$v = f(\eta),\ u = -\frac{r}{2}f'(\eta). \quad (4)$$

Eliminating ρ from (1) and differentiating the resulting equation with respect to η we get

$$f^{4'} - Rff''' + RS(4f''f''' - ff^{5'} + f'f^{4'}) = 0. \quad (5)$$

and boundary conditions become

$$f' = 0,\ f = V_1,\ \theta = 0 \text{ at } \eta = -1$$
$$f' = 0,\ f = V_2,\ \theta = 1 \text{ at } \eta = 1. \quad (6)$$

3. METHOD OF SOLUTION

Equation (5) is a 5th-order differential equation and it is difficult to have a closed form solution with four boundary conditions. If we put $S = 0$, it reduces to an equation governing the Newtonian fluid. Hence we can regard the effect of elasticity as a perturbation over the Newtonian fluid. Moreover, when $R = 0$, the elasticity of the fluid does not play any role. Thus we take R as a perturbation parameter for small injection or suction rate and write

$$f(\eta) = \sum_{n=0}^{\infty} R^n f_n(\eta). \quad (7)$$

Substituting (7) into equation (5) and equating like powers up to the coefficient of R^2 we get three equations, and solving these with appropriate boundary conditions we get

$$f(\eta) = \frac{1}{4}(V_1 - V_2)(\eta^3 - 3\eta) + \frac{1}{2}(V_1 + V_2) + R\left[\frac{(V_1 - V_2)^2}{2240}(\eta^7 - 21\eta^5 + 39\eta^3 + 9\eta) - \frac{3S}{40}(V_1 - V_2)^2 \times (\eta^5 - 2\eta^3 + \eta) + \frac{1}{32}(V_1^2 - V_2^2)(\eta^4 - 2\eta^2 + 1)\right]. \quad (8)$$

The expression for f_2 is not included as it is very large. The dimensionless skin frictions at the plates $\eta = -1$ and $\eta = 1$ are given by

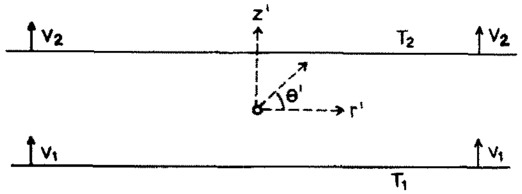

FIG. 1. Geometry of the problem.

$$\tau|_{\eta=-1} = -\frac{3}{2}(V_1 - V_2) + \frac{R}{4}\left[\frac{9}{35}(V_1 - V_2)^2 + (V_1^2 - V_2^2)\right] - \frac{3}{20}RS[(V_1 - V_2)^2 + 5(V_1^2 - V_2^2)] \quad (9)$$

and

$$\tau|_{\eta=1} = \frac{3}{2}(V_1 - V_2) + \frac{R}{4}\left[(V_1^2 - V_2^2) - \frac{9}{35}(V_1 - V_2)^2\right] + \frac{3}{20}RS[(V_1 - V_2)^2 - 5(V_1^2 - V_2^2)]. \quad (10)$$

Substitution of (4) into equation (3) gives

$$f\frac{\partial \theta}{\partial \eta} - rf'\frac{\partial \theta}{\partial r} = \frac{1}{PR}\left(\frac{\partial^2 \theta}{\partial r^2} + \frac{1}{r}\frac{\partial \theta}{\partial r} + \frac{\partial^2 \theta}{\partial \eta^2}\right) + \frac{E}{R}\left(3f'^2 + \frac{r^2}{4}f''^2\right) - \frac{SE}{2}\left(6ff'f'' - 6f'^3 - \frac{3}{2}r^2f'f''^2 + \frac{r^2}{2}ff''f'''\right). \quad (11)$$

In view of equation (11), θ can be written in the form

$$\theta = r^2\theta_2(\eta) + \theta_0(\eta). \quad (12)$$

From (12) and (11), the following equations are obtained:

$$-f\theta_2 + f\theta'_2 = \frac{\theta''_2}{PR} + \frac{E}{4R}f''^2 + \frac{SE}{4R}(3f'f''^2 - ff''f''') \quad (13)$$

and

$$f\theta'_0 = \frac{1}{PR}(4\theta_2 + \theta''_0) + \frac{3E}{R}f'^2 + 3SE(f'^3 - ff'f'')$$

which are to be solved with the conditions

$$\eta = -1:\ \theta_2 = \theta_0 = 0$$
$$\eta = 1:\ \theta_2 = 0,\ \theta_0 = 1. \quad (14)$$

Let us write

$$\theta_2 = \theta_{2,0} + V_1\theta_{2,1} + V_2\theta_{2,2} + V_1^2\theta_{2,11} + V_1V_2\theta_{2,12} + V_2^2\theta_{2,22} + \ldots$$
$$\theta_0 = \theta_{0,0} + V_1\theta_{0,1} + V_2\theta_{0,2} + V_1^2\theta_{0,11} + V_1V_2\theta_{0,12} + V_2^2\theta_{0,22} + \ldots \quad (15)$$

and

$$f = V_1F_1 + V_2F_2 + V_1^2F_{11} + V_1V_2F_{12} + V_2^2F_{22} + \ldots.$$

Substitution of (15) into (13) gives two sets of differential equations which when solved with proper boundary conditions lead to

$$\theta = \frac{3}{64}r^2PE(V_1 - V_2)^2(1 - \eta^4) + \frac{1}{2}(\eta + 1) - \frac{PR}{160}V_1(1 - \eta^2)(20 - 9\eta + \eta^3) - \frac{V_2PR}{160}(1 - \eta^2) \times (20 + 9\eta - \eta^3) + V_1^2(1 - \eta^2)\left[\frac{PE}{160}(113 - 37\eta^2 + 8\eta^4) - \frac{PR^2}{1612800}(9240 - 613\eta - 3360\eta^2 + 527\eta^3 + 840\eta^4 - 175\eta^5 + 5\eta^7) + \frac{P^2R^2}{1612800}(10920 - 32209\eta + 33600\eta^2 - 9949\eta^3 - 4200\eta^4 + 2525\eta^5 - 175\eta^7) + \frac{SPR^2}{11200}(10\eta^5 - 32\eta^3 + 38\eta)\right] + V_2^2(1 - \eta^2) \times \left[\frac{PE}{160}(113 - 37\eta^2 + 8\eta^4) + \frac{PR^2}{1612800}(9240 + 613\eta - 3360\eta^2 - 527\eta^3 + 840\eta^4 + 175\eta^5 - 5\eta^7)\right.$$

$$- \frac{P^2R^2}{1612800}(10920 + 32209\eta + 33600\eta^2 + 9949\eta^3 - 4200\eta^4 - 2525\eta^5 + 175\eta^7) + \frac{SPR}{11200}(10\eta^5 - 32\eta^3 + 38\eta)\Bigg] - V_1V_2(1-\eta^2)\Bigg[\frac{PE}{80}(113 - 37\eta^2 + 8\eta^4) + \frac{PR^2}{806400}(613\eta - 527\eta^3 + 175\eta^5 - 5\eta^7) + \frac{P^2R^2}{806400}(34991\eta - 9949\eta^3 + 2525\eta^5 - 175\eta^7) + \frac{SPR^2}{5600}(10\eta^5 - 32\eta^3 + 38\eta)\Bigg]. \quad (16)$$

The Nusselt number q at the lower disc and at the upper disc is respectively given by

$$q|_{\eta=-1} = -\frac{3}{16}PEr_0^2(V_1 - V_2)^2(\lambda^2 + 1) - 2\Bigg[\frac{1}{2} - \frac{7}{20}V_1P - \frac{3}{20}V_2P + V_1^2\left(\frac{21}{20}PE - \frac{109}{12600}PR + \frac{313}{3150}P - \frac{SPR}{350}\right) + V_2^2\left(\frac{21}{20}PE + \frac{101}{12600}PR - \frac{P^2}{1575} - \frac{SPR}{350}\right) - V_1V_2\left(\frac{21}{10}PE - \frac{PR}{1575} - \frac{107P^2}{1575} - \frac{SPR}{175}\right)\Bigg] \quad (17)$$

and

$$q|_{\eta=1} = \frac{3}{16}PE(V_1 - V_2)^2r_0^2(\lambda^2 + 1) - 2\Bigg[\frac{1}{2} + \frac{3}{20}V_1P + \frac{7}{20}V_2P - V_1^2\left(\frac{21}{20}PE - \frac{101}{12600}PR + \frac{P^2}{1575} + \frac{SPR}{350}\right) + V_1V_2\left(\frac{21}{10}PE + \frac{PR}{1575} + \frac{107}{1575}P^2 + \frac{SPR}{175}\right) - V_2\left(\frac{21}{20}PE + \frac{109}{12600}PR - \frac{313}{3150}P^2 + \frac{SPR}{350}\right)\Bigg] \quad (18)$$

where

$$\lambda = \frac{r}{r_0}.$$

4. DISCUSSION

Figures 2 and 3 represent the axial velocity distribution for different values of S, R, V_1 and V_2. For a fixed value of V_2, the velocity decreases with respect to η. The elasticity of the liquid decreases it further up to the central plane after which an opposite effect is observed. The same conclusion may be drawn when $V_1 > V_2$. A reverse effect is seen in the case if $V_1 < V_2$. It is very interesting to observe that the velocity is independent of the effect of elasticity at any point on the central plane. All the curves are symmetrical with respect to the central plane. The velocity decreases as R increases in the region $(-1, 0)$ for $V_1 > V_2$, but increases for $V_1 < V_2$. An opposite nature is observed in the interval $(0, 1)$.

The radial velocity is depicted in Fig. 4. When $V_1 = 0.4$ and $V_2 = 0.2$, the velocity increases from zero at the lower disc to the central plane and then decreases from the central plane to the upper disc. When $V_1 = 0.4$ and $V_2 = -0.2$, the velocity is more than the corresponding parts, when $V_1 = 0.4$, and $V_2 = 0.2$. When there is suction at both the discs, an opposite nature is noticed. The effect of elasticity is to decrease the velocity near the two discs but to increase the velocity near the central plane. The figure is not sensitive enough to indicate this observation.

The shearing stress (Fig. 5) at $\eta = 1$ decreases as R increases for all values of V_1 and V_2. The elastic elements in the liquid increase the shearing stress at every point. An opposite effect is observed at the disc $\eta = -1$.

The temperature (Fig. 6) increases with the increase in the values of both P and E. When there is fluid injection at the lower disc and fluid suction at the upper disc, θ rises from zero at the lower disc to one at the upper disc, remaining greater than one throughout the region of the fluid except in the neighbourhood of the lower disc. When there is suction at both the discs and at every point of the fluid, θ is more than its

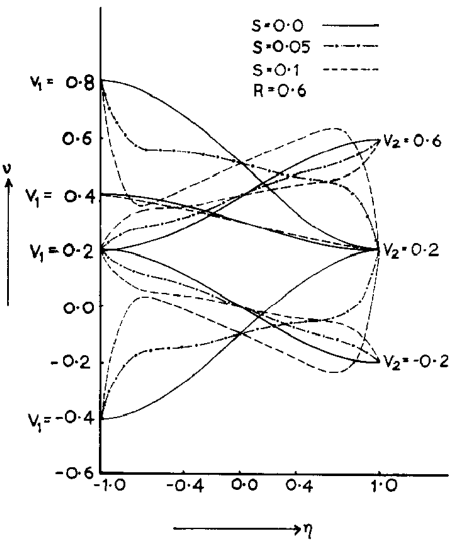

FIG. 2. Axial velocity distribution for different values of S, V_1 and V_2.

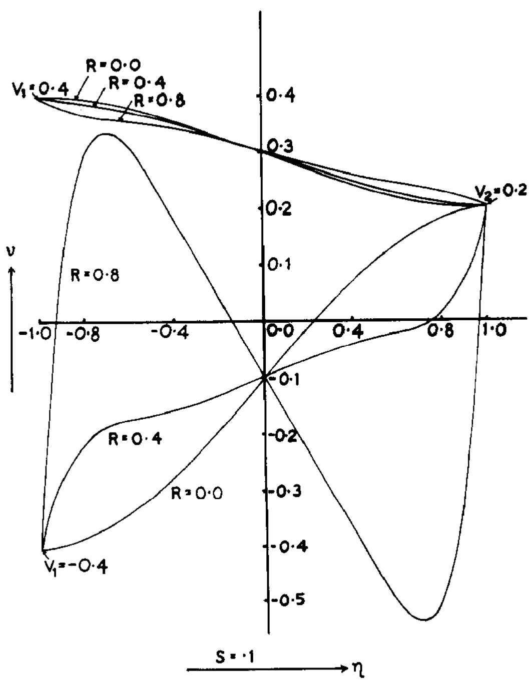

FIG. 3. Effect of R, V_1 and V_2 on v.

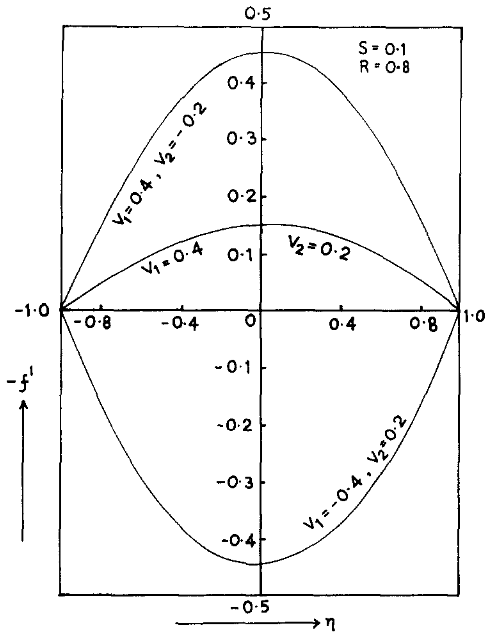

FIG. 4. Effect of V_1 and V_2 on $(-f')$.

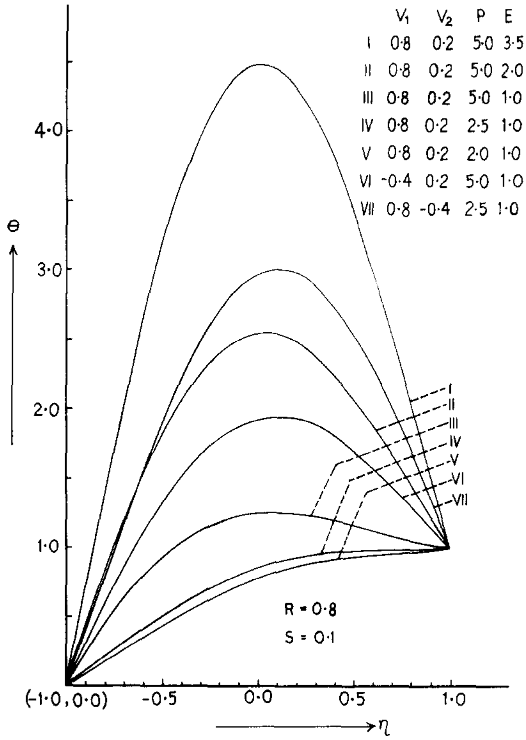

FIG. 6. Temperature distribution for different values of V_1, V_2, P and E.

corresponding part for $V_1 > 0$ and $V_2 > 0$. There is a sharp rise in the value of θ when there is fluid injection at both the discs. For all the profiles, the maximum temperature moves towards the upper disc. The temperature decreases as R increases, and the effect of elasticity on θ is very small. The elasticity of the liquid decreases the fluid temperature between the lower disc and central plane and increases the value of θ from the central plane to the upper disc (Table 1).

The rates of heat transfer at both the discs are shown in Fig. 7. The rate of heat transfer at the upper disc increases in some liquid layer due to an increase in the value of both P and E; outside that layer an opposite effect is observed. For a fixed $V_1 > 0$, $q|_{+1}$ decreases as $V_2 > 0$ increases. When there is fluid injection at both discs, $q|_{+1}$ is more than that of when $V_1 > 0$ and $V_2 > 0$. The value of $q|_{+1}$ decreases with an increase in λ. A reverse phenomenon is noticed at the lower disc. The effect of elasticity is to increase the rate of heat transfer at both discs.

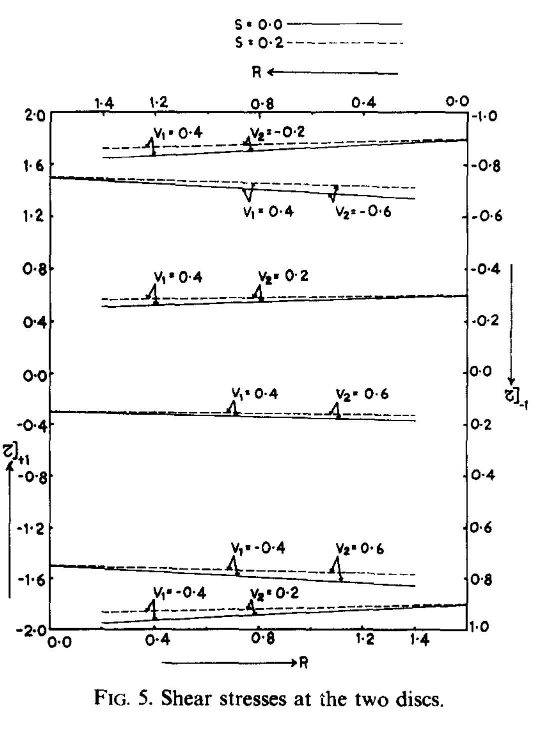

FIG. 5. Shear stresses at the two discs.

Acknowledgement—The authors express their sincere thanks to the referee for his valuable suggestions.

Table 1. Values for θ for different values of R and S.

η/R	0.2	0.8	1.0	S
	0.00000	0.00000	0.00000	0.0
-1.0	0.00000	0.00000	0.00000	0.1
	0.58374	0.57994	0.57867	0.0
-0.6	0.58372	0.57984	0.57855	0.1
	1.01499	1.00869	1.00659	0.0
-0.2	1.01498	1.00863	1.00651	0.1
	1.14280	1.13620	1.13400	0.0
0.0	1.14280	1.13620	1.13400	0.1
	1.20396	1.19777	1.19571	0.0
0.2	1.20398	1.19784	1.19579	0.1
	1.15571	1.15207	1.15085	0.0
0.6	1.15573	1.15217	1.15098	0.1
	1.00000	1.00000	1.00000	0.0
1.0	1.00000	1.00000	1.00000	0.1

$V_1 = 1.0$, $V_2 = 0.2$, $r = 0.5$, $P = 2.0$, $E = 1.0$.

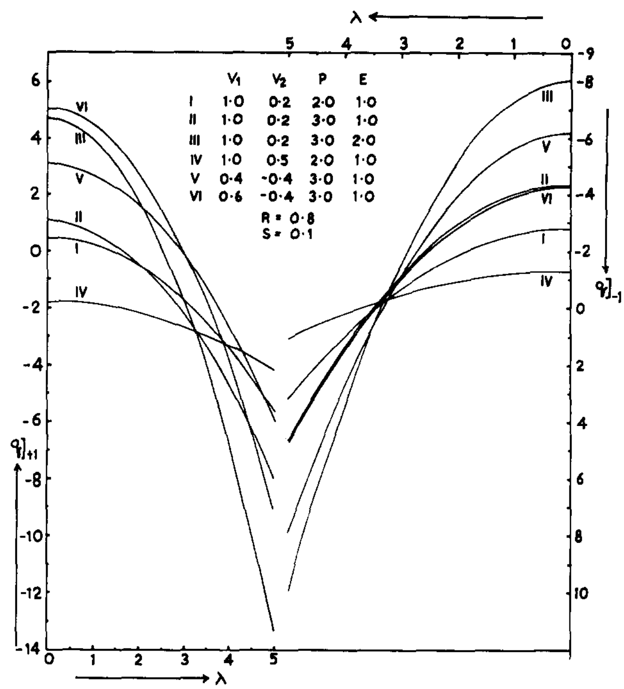

FIG. 7. Rate of heat transfer at the discs.

REFERENCES

1. A. F. Elkouh, Laminar flow between rotating porous disks, *J. Engng Mech. Div. Proc. Am. Soc. Civil Engrs* **4**, 919 (1968)
2. S. P. Mishra, B. P. Acharya and J. Sinha Roy, Laminar elastico-viscous flow between rotating porous disks, *Rev. Roum. Sci. Tech. Mech. Appl.* **20**, 257 (1975).
3. H. Rasmussen, Steady viscous flow between two porous disks. *ZAMP* **21**, 187 (1970).
4. C. Y. Wang, Steady symmetric flow between two rotating porous disks, *Q. appl. Math.* **34**, 29 (1976).
5. R. M. Terril and J. P. Cornish, Radial flow of a viscous, incompressible fluid between two stationary uniformly porous disks, *ZAMP* **24**, 676 (1973).
6. K. Walters, The solutions of flow problems in the case of materials with memory I. *J. Mécanique* **1**, 479 (1962).

Int. J. Heat Mass Transfer. Vol. 25, No. 7, 1069–1071, 1982
Printed in Great Britain
0017-9310/82/071069-03 $03.00/0

EVALUATION OF THE GEOMETRIC MEAN TRANSMITTANCE AND TOTAL ABSORPTANCE FOR TWO-DIMENSIONAL SYSTEMS

W. W. YUEN

Department of Mechanical and Environmental Engineering, University of California, Santa Barbara, CA 93016, U.S.A.

(*Received* 23 *June* 1981 *and in revised form* 18 *November* 1981)

NOMENCLATURE

a_λ,	absorption coefficient;
A_1, A_2,	area elements;
D,	length defined in Fig. 3;
E_n,	exponential function;
$F(x, 1/2^{1/2})$,	elliptic function of the first kind;
F_{i-j},	shape factor between areas A_i and A_j;
H,	$(R^2 + z^2)^{1/2}$;
$\mathbf{n}_1$, $\mathbf{n}_2$,	unit vectors defined in Fig. 1;
$\mathbf{r}_1$,	unit vector defined in Fig. 1;
r,	distance between dA_1 and dA_2;
R,	length defined in Fig. 2;
R_{i-j},	weak-band geometric mean beam length;
S_{i-j},	strong-band geometric mean beam length;
W_{i-j},	very-strong-band geometric mean beam length;
θ,	angle defined in Fig. 2;
ϕ,	angle defined in Fig. 3;
$\tau_{\lambda,d1-2}$,	geometric-mean transmittance.